31st Congress of the International Council of the Aeronautical Sciences

Belo Horizonte, Brazil; September 09-14, 2018

A COMPARISON BETWEEN UNIVERSAL INTEGRAL REGULATOR AND LINEAR QUADRATIC TECHNIQUE FOR AN AIRCRAFT AUTOPILOT

Yohan Díaz-Méndez* Marcelo Santiago de Sousa* Sebastião Simões Cunha Jr* , Guilherme Ferreira Gomes*

***Department of Mechanical Engineering, Federal University of Itajubá, BPS avenue, 1303, Itajubá, Brazil**

Keywords: *Universal Integral Regulator, Linear Quadratic Regulator, Flight Control, Nonlinear Control, Sliding Mode Control*

Abstract

This paper considers a comparative assessment based on time response performance between a robust nonlinear control technique Universal Integral Regulator (UIR) and the modern and well-known linear technique Linear Quadratic Regulator (LQR) for the velocity tracking control of a nonlinear aircraft model. The UIR is based on sliding mode control design but using a conditional integrator in order to improve the transient response of the controller and to maintain the tracking error at zero. On the other hand, the LQR have demonstrated to be a powerful technique used to perform systematically gain scheduling at various flight conditions in linearized aircraft models. The control objective is to determine the elevator deflection to asymptotically track desired reference for the velocity. Results demonstrated a better performance using UIR controller, providing smaller tracking error, less control activity and more robustness.

1 Introduction

The development of aircraft controllers have been the focus of many researchers in the past and this area is continuously growing in order to attend the civilian and military new projects. Controllers help pilots in stabilizing the aircraft and serve as a back up source of control in the case of a flight surface failure. In military applications, the tracking of a target or simply the proper control of the commonly unstable dynamic require robust and effective controllers. Due to the abrupt maneuvers and huge flight envelope of this kind of aircraft, a linearized model and gain scheduling technique will require a lots of gain adjustments (computations) during the whole flight, consuming time at expense of computational cost. A robust controller can minimize the computations and provide a set of controller gains that could be valid at any point of the flight envelope.

Many control methods have been used in flight control, among them we have: Proportional Integrative Derivative (PID) controller sucessfully implemented in [1] and [8] in which Genetic Algorithm (GA) optimization was used to tune the PID gains. Linear Quadratic Regulator (LQR) also was considered to control maneuvers in a flexible aircraft in [18], aircraft trajectory in conjunction with Nonlinear Dynamic Inversion (NDI) in [13], hypersonic flight in [11], flight stability in the LSU-05 unmanned aerial vehicle in [9] and is one of the most implemented techniques in the aeronautical industry [4].

According to [11], the design of a robust controller for a real world application using a nonlinear model is a challenging task. In the literature some methods have been proposed, the most

commonly used, as mentioned above, require a linearized model whose linear matrices need to be updated at a given operating point in the flight envelope. Then, the feedback linearization (FL) technique helped to eliminate the need of gain scheduling and some techniques based on FL begins to be studied. One of these techniques is the Sliding Mode Controller (SMC) which was successfully applied in flight control in the works of [19], [10] and [2].

The Universal Integral Regulator (UIR) is based on the SMC technique, it was created by Hassan Khalil in the work [5] and improved by his co-workers in subsequent works as [6], [12] and others. As mentioned before, UIR is a SMC based technique which enhanced transient response by means of a conditional integrator. UIR can be easily implemented and its controller parameters can be obtained analytically through a mathematical and simple stability analysis (at least in this paper).

In the present work the UIR and the LQR techniques are applied to the velocity tracking of a fighter aircraft modeled with the aerodynamic, mass, and inertia properties of a *Mirage III* aircraft. The control objective is to determine the elevator deflection to asymptotically track desired reference for the velocity. Performance of both controller are compared.

2 Aircraft Model

The aircraft dynamic considered in this work is the longitudinal model of a Mirage III fighter aircraft extracted from [15]. The three-degrees-of-freedom mathematical model uses aerodynamic data (stability and control derivatives) which can be considered approximately constant (independent of the equilibrium point). The model in a combined wind and body axes is described as:

$$\begin{aligned}
\dot{V} &= \frac{1}{V}(u\dot{u} + v\dot{v} + w\dot{w}) \\
\dot{\alpha} &= \frac{\left(\frac{\dot{w}}{u} - \frac{w\dot{u}}{u^2}\right)}{\sqrt{1+(w/u)^2}} \\
\dot{q} &= c_5 pr - c_6(p^2 - r^2) + c_7 M \\
\dot{\Theta} &= qcos\Phi - rsen\phi
\end{aligned} \tag{1}$$

Where, V is the total velocity of the aircraft, α is the angle of attack, q the pitch rate, Θ the attitude angle and the constants $c_5 = (I_{zz} - I_{xx})/I_{yy}$, $c_6 = I_{xz}/I_{yy}$ and $c_7 = 1/I_{yy}$. In this work, it is assumed that the longitudinal and latero-directional dynamics are decoupled and the latero-directional variables Φ, p and r are approximately zero. The equations of motion of the velocity components u, v and w are represented as follows:

$$\begin{aligned}
\dot{u} &= m^{-1}(F_x + Tcos\alpha_f) - gsen\phi \\
&\quad + rv - qw \\
\dot{v} &= m^{-1}F_y + gsen\phi cos\theta \\
&\quad + pw - ru \\
\dot{w} &= m^{-1}(F_z + Tsen\alpha_f) + gcos\phi cos\theta \\
&\quad + qu - pv
\end{aligned} \tag{2}$$

Where m is the aircraft mass, g the acceleration of gravity, T the maximum thrust and α_f the engine incidence angle considered null in this work. The forces F_x, F_y, F_z and the pitch moment M are written as:

$$\begin{aligned}
F_x &= \bar{q}SC_x \quad F_y = \bar{q}SC_y \\
F_z &= \bar{q}SC_z \quad M = \bar{q}S\bar{c}C_m
\end{aligned} \tag{3}$$

Where $\bar{q}$ denotes the dynamic pressure and S and $\bar{c}$ the wing surface and mean aerodynamic chord respectively. The aerodynamic coefficients C_x, C_y, C_z and C_m are function of the Euler angles and the aerodynamic coefficients C_L, C_D and C_ya which in turn depend on the stability derivatives C_{m_0}, C_{m_α}, C_{m_q}, control derivative $C_{m_{\delta_p}}$ and control input δ_p. Some physical properties and

Table 1 aircraft properties

Property	Value	Property	Value
$m[kg]$	7400	C_{L_q}	0
$S[m^2]$	36	C_{m_0}	0
$\bar{c}[m]$	5.25	C_{m_α}	-0.17
$I_{yy}[kg \cdot m^2]$	5.4×10^4	C_{m_q}	-0.4
C_{L_0}	0	$C_{m_{\delta p}}$	-0.45
C_{L_α}	2.204	-	-

aerodynamic data of the model are showed in Table 1.

Expanding Equation 1 and using Equations 2 and 3 the system can be written in as:

$$\begin{aligned}
\dot{V} &= g\sin(\alpha-\Theta)+\frac{T}{m}\cos\alpha \\
&\quad -\frac{\bar{q}S}{m}C_d(\alpha,q)+\left(\frac{T}{m}\cos\alpha\right)\delta_\pi \\
\dot{\alpha} &= q+\frac{g}{V}\cos(\alpha-\Theta)-\frac{T}{mV}\sin\alpha \\
&\quad +\frac{\bar{q}S}{mV}C_L(\alpha,q)-\left(\frac{T}{mV}\sin\alpha\right)\delta_\pi \\
\dot{q} &= \frac{\bar{q}S\bar{c}}{I_{yy}}\left[C_{m_0}+C_{m_\alpha}\alpha+C_{m_q}\left(\frac{\bar{c}}{V}\right)q\right] \\
&\quad +\left(\frac{\bar{q}S\bar{c}}{I_{yy}}C_{m_{\delta_p}}\right)\delta_p \\
\dot{\Theta} &= q
\end{aligned} \tag{4}$$

3 Controller Design-Universal Integral Regulator

The UIR controller developed in this section is based on the work of [12], the assumptions taken into account will be mentioned throughout the controller design.

3.1 Problem Formulation

Consider the system in Equation 4. This system can be rewritten in the input affine-form $\dot{x} = f(x)+g(x)u$ with the state vector $x \in R^n$ $(n=4)$ as $x=\{V,\alpha,q,\Theta\}^T$, the control input vector $u \in R^m$ $(m=1)$ as $u=\{\delta_p\}$, and the output vector $y \in R^p$ $(p=m)$ as $y=h(x)=V$. With the smooth functions $f(x)=[f_1,f_2,f_3,f_4]^T$ and $g(x)=[g_1,g_2,g_3,g_4]^T$ as showed in Equation 5.

$$f(x)=\begin{bmatrix} g\sin(\alpha-\Theta)+\frac{T}{m}\cos\alpha \\ -\frac{\bar{q}S}{m}C_d(\alpha,q)+\left(\frac{T}{m}\cos\alpha\right)\delta_\pi \\ q+\frac{g}{V}\cos(\alpha-\Theta)-\frac{T}{mV}\sin\alpha \\ +\frac{\bar{q}S}{mV}C_L(\alpha,q)\left(\frac{T}{mV}\sin\alpha\right)\delta_\pi \\ \frac{\bar{q}S\bar{c}}{I_{yy}}\left[C_{m_0}+C_{m_\alpha}\alpha+C_{m_q}\left(\frac{\bar{c}}{V}\right)q\right] \\ q \end{bmatrix} \tag{5}$$

$$g(x)=\begin{bmatrix} 0 \\ 0 \\ \frac{\bar{q}S\bar{c}}{I_{yy}}C_{m_{\delta_p}} \\ 0 \end{bmatrix}$$

The control problem consists in designing the elevator control input that makes the total velocity of the aircraft V to track a "ramp" type reference from one equilibrium velocity to another. According to [12] the control problem can be solved if the internal dynamic of the system is input-to-state stable, in this work is assumed that the internal dynamic attends this criterion. In order to better formulate the control problem is assumed that the system has uniform relative degree and can be converted to normal form (assumption 1 in [12]). Another assumption considered in this work in order to simplify the control problem, as mentioned before, is that all the latero-directional state variables are null or constant and only the longitudinal states are time varying, therefore, the longitudinal and latero-directional dynamics are decoupled.

3.2 Relative Degree, Normal Form Transformation and Tracking Problem

Using the first assumption and the Lie derivative of Equation 6 as proposed in [14] and [5], we can compute the relative degree to the output $y=h(x)=V$, then, for $k=0$ we have (see Equation 7 :

$$L_{g_j}L_f^k h_i(x)=0, \qquad \begin{matrix} 0\le k\le \rho_i-2 \\ 0\le i,j\le m \end{matrix} \tag{6}$$

$$L_g L_f^0 h(x) = L_g h(x) = \begin{bmatrix} \frac{\partial h}{\partial x_1} & \frac{\partial h}{\partial x_2} & \frac{\partial h}{\partial x_3} & \frac{\partial h}{\partial x_4} \end{bmatrix} \begin{bmatrix} g_1 \\ g_2 \\ g_3 \\ g_4 \end{bmatrix} \tag{7}$$

With $L_g h(x) = 0$ due to $g_1 = g_2 = g_4 = 0$ and h does not depend on x_3, therefore, $k = 0$ does not attend Equation 6. for $k = 1$, the Lie derivative becomes:

$$L_g L_f^1 h(x) = \frac{\partial f_1}{\partial x_3} g_3 \tag{8}$$

Then, $L_g L_f h(x) = 0$, because f_1 does not depend on $x_3 = q$. Using $k = 2$, we have:

$$L_g L_f^2 h(x) = \frac{\partial \bar{A}}{\partial x_3} g_3 \tag{9}$$

with $\bar{A} = \frac{\partial f_1}{\partial x_2} f_2 + \frac{\partial f_1}{\partial x_4} f_4$. Solving Equation 9 with $x_3 = q$ we obtain:

$$L_g L_f^2 h(x) = -\frac{T}{m} sen\alpha(1 + \delta_\pi) \neq 0 \tag{10}$$

Resulting in a relative degree $\rho = k + 1 = 3$. Due to $\rho < n$ the transformation to normal form is partial and we have internal and external dynamics represented, respectively, by the new variables η and ξ.

3.3 New Variables

The new internal and external variables are determined by mean of the Equations 11 and 12. The new external variables are computed in Equation 13.

$$\xi_j^i = L_f^{j-1} h_i \quad \begin{cases} 1 \leq j \leq \rho \\ 1 \leq i \leq m \end{cases} \tag{11}$$

$$L_g \eta = 0 \tag{12}$$

$$\begin{aligned} \xi_1 &= L_f^0 h(x) = h(x) = V \\ \xi_2 &= L_f h(x) = f_1 = g \sin(\alpha - \Theta) + \frac{T}{m} \cos\alpha \\ &\quad - \frac{\bar{q} S}{m} C_d(\alpha, q) + \left(\frac{T}{m} \cos\alpha \right) \delta_\pi \\ \xi_2 &= L_f^2 h(x) = \bar{A} \end{aligned} \tag{13}$$

With f_1, f_2, f_3 and f_4 as defined in Equation 5. It is easy to check that the simplest choice $\eta = \Theta$ satisfy the condition in Equation 12, this, by the fact that $g_1 = g_2 = g_4 = 0$ and the choice of η does not depend on q (see Equation 14).

$$L_g \eta = \frac{\partial \eta}{\partial V} g_1 + \frac{\partial \eta}{\partial \alpha} g_2 + \frac{\partial \eta}{\partial q} g_3 + \frac{\partial \eta}{\partial \Theta} g_3 = 0 \tag{14}$$

3.4 New Dynamic (Normal Form)

In accordance with [5] the new external and internal dynamics are constructed as in Equations 15 and 17 respectively, then, the normal form transformation is completed, the computing of the function $b(x)$ was done with a software aid and due to space limitations is not presented here.

$$\begin{aligned} \dot{\xi_1} &= \xi_2 \\ \dot{\xi_2} &= \xi_3 \\ \dot{\xi_3} &= b(x) + a(x)u \end{aligned} \tag{15}$$

Where:

$$b(x) = L_f^3 h(x) = \begin{bmatrix} \frac{\partial \bar{A}}{\partial x_1} & \frac{\partial \bar{A}}{\partial x_2} & \frac{\partial \bar{A}}{\partial x_3} & \frac{\partial \bar{A}}{\partial x_4} \end{bmatrix} \begin{bmatrix} f_1 \\ f_2 \\ f_3 \\ f_4 \end{bmatrix}$$

$$a(x) = L_g L_f^2 h(x) = A(x) = -\frac{T}{m} sen\alpha(1 + \delta_\pi) \tag{16}$$

$$L_f \eta = f_4 = \dot{\Theta} = q \tag{17}$$

3.5 Tracking problem

Through assumption 2 in [12] it is possible to define the error dynamics. Let $z = \eta - \bar{\eta}$ be the internal dynamic error with $\bar{\eta} = \Theta_{eq}$ and $e_i = \xi_i - \bar{\xi}_i - v_1$ the external dynamic error with $\bar{\xi}_1 = [r_{1ss}, 0, 0] = [V_{eq}, 0, 0]$ and $v_1 = [r_1 - r_{1ss}, r_1^{(1)}, r_1^{(2)}] = [V_{ref} - V_{eq}, V_{ref}^{(1)}, V_{ref}^{(2)}]$ where $V_{ref}^{(1)}$ and $V_{ref}^{(2)}$ are respectively the first and the second time derivative of the velocity reference. Finally, the system error is as showed in Equation 18 and the error dynamics can be written in the compact matrix form as in Equation 19.

$$e = [e_1^V, e_2^V, e_3^V] = [\xi_1 - V_{ref}, \xi_2 - V_{ref}^{(1)}, \xi_3 - V_{ref}^{(2)}] \tag{18}$$

$$\begin{Bmatrix} \dot{e}_1^V \\ \dot{e}_2^V \\ \dot{e}_3^V \end{Bmatrix} = \begin{bmatrix} 0 & 1 & 0 \\ 0 & 0 & 1 \\ 0 & 0 & 0 \end{bmatrix} \begin{Bmatrix} e_1^V \\ e_2^V \\ e_3^V \end{Bmatrix} + \begin{bmatrix} 0 \\ 0 \\ 1 \end{bmatrix} \{b(x) + a(x)u\} \tag{19}$$

3.6 RIU Controller

The first step to be acomplished is to design the sliding surface of a Continuous Sliding Mode Controller (CSMC) (Equation 20) modified by the introduction of a conditional integrator (see Equation 22 whose variable is defined as σ_V. Using the relative degree previously computed $\rho = 3$, it is possible to obtain Equation 21.

$$s_V = k_0^V \sigma_V + \sum_{j=1}^{\rho-1} k_j^V e_j^V + e_\rho^V \quad 1 \leq j \leq \rho - 1 \tag{20}$$

$$s_V = k_0^V \sigma_V + k_1^V e_1^V + k_2^V e_2^V + e_3^V \tag{21}$$

$$\dot{\sigma}_V = -k_0^V \sigma_V + \mu_V sat\,(s_V/\mu_V) \tag{22}$$

Where $e_2^V = \dot{e}_1^V$ and $e_3^V = \dot{e}_2^V$. The constants $k_1^V, k_2^V > 0$ are chosen such that the polynomial $k_1^V + k_2^V \lambda^1 + \lambda^2 = 0$ has only roots (λ) with negative real parts (Hurwitz). Deriving the sliding surface we have:

$$\dot{s}_V = k_0^V \dot{\sigma}_V + k_1^V e_2^V + k_2^V e_3^V + \dot{e}_3^V \tag{23}$$

Using the conditional integrator dynamics defined in Equation 22 and using $\dot{e}_3^V$ from Equation 19, we get:

$$\dot{s}_V = k_0^V \left\{ -k_0^V \sigma_V + \mu_V sat\,(s_V/\mu_V) \right\} + k_1^V e_2^V + k_2^V e_3^V + b(x) + a(x)u_V \tag{24}$$

Assuming that $a(x) = A(x)$ is completely known, we define the UIR controller as in [12]:

$$\begin{cases} u_V = a(x)^{-1} \left[-\hat{F}_V(\cdot) + v_V \right] \\ v_V = -K_V sat\left(\frac{s_V}{\mu_V}\right) \end{cases} \tag{25}$$

With $F_V(\cdot) = k_1^V e_2^V + k_2^V e_3^V + b(x)$ and $\hat{F}_V(\cdot)$ a nominal value of $F_V(\cdot)$. Due to the flexibility of choosing $\hat{F}_V(\cdot) = 0$ for SISO systems (see [12] for more details), the controller will be of the form:

$$u_V = -a(x)^{-1} K_V sat\left(\frac{s_V}{\mu_V}\right) \tag{26}$$

With $K_V = \nu_V(\cdot) + q_V$ and $q_V > 0$ as stated in assumption 6 of [12]. Substituting u_V in $\dot{s}_V$ of Equation 24 and analyzing outside the boundary layer ($|s_V| \geq \mu_V$), in this region $sat\,(s_V/\mu_V) = s_V/|s_V|$, then:

$$\dot{s}_V = \Delta_V(\cdot) - K_V(s_V/|s_V|) \tag{27}$$

Where:

$$\Delta_V(\cdot) = k_0^V \left\{ -k_0^V \sigma_V + \mu_V sat\,(s_V/\mu_V) \right\} + F_V(\cdot) \tag{28}$$

It is easy to demonstrate in a simple stability analysis for s_V that choosing the Candidate Lyapunov Function (CLF) $V_s = \frac{1}{2} s_V^2$, its first derivative will be $\dot{V}_s = s_V \dot{s}_V$ which will be $\dot{V}_s < 0$ if we define $\nu_V(\cdot)$ as in Equation 29.

$$\nu_V(\cdot) \geq max\left|\Delta_V(\cdot)\frac{|s_V|}{s_V}\right| \tag{29}$$

Maximizing the last equation we have:

$$\begin{aligned}\Delta_V(\cdot) &= \frac{|s_V|}{s_V}k_0^V\left\{-k_0^V\sigma_V + \mu_V\frac{s_V}{|s_V|}\right\} + \frac{|s_V|}{s_V}F_V(\cdot)\\ &= -\left(k_0^V\right)^2\sigma_V\frac{|s_V|}{s_V} + k_0^V\mu_V + \frac{|s_V|}{s_V}F_V(\cdot)\\ &\leq k_0^V\mu_V - sign(s_V)k_0^V\mu_V + \frac{|s_V|}{s_V}F_V(\cdot)\\ &\leq 2k_0^V\mu_V + |F_V(\cdot)|\end{aligned} \tag{30}$$

We choose $q_V = 2.1k_0^V\mu_V > 0$ to cancel the term $2k_0^V\mu_V$ and $\nu_V(\cdot)$ needs to be $\nu_V(\cdot) \geq |F_V(\cdot)| = k_1^V\left|e_2^V\right| + k_2^V\left|e_3^V\right| + |b(x)|$. Finally we determine the controller gain by means of $K_V = \nu_V(\cdot) + q_V$ with $k_1^V > 0$ and $k_2^V > 0$ as stated in the first part of the RIU controller, establishing maximum tracking errors for e_2^V and e_3^V and computing $|b(x)|$ as in Equation 16.

4 Controller Design-Linear Quadratic Regulator (LQR)

In order to apply the LQR controller to the tracking problem of the aircraft velocity it is necessary re-define the system states and outputs in order to simplify the nomenclature. Based on the theory presented in [17] for LQR controllers, the aircraft dynamic needs to be linearized in several operating points and then LQR gains are scheduled. In this work, the linearization is done using the small perturbation theory and once the linear matrices are obtained we proceed to construct the augmented dynamic as in [17], that is, *aircraft+actuator+compensator*, whose total dynamic is written as:

$$\begin{cases}\dot{x} = Ax + Bu + Gr\\ y = Cx + Fr\\ z = Hx\end{cases} \tag{31}$$

With $z(t)$ as the performance output (different from the measured output $y(t)$). Output is desired to follow the reference r. F and G are matrices chosen to introduce the desired structure of the dynamic compensator $\dot{w}$ which is defined as:

$$\begin{cases}\dot{w} = Fw + Ge\\ v = Dw + J_c e\end{cases} \tag{32}$$

Whose input is the tracking error $e = r(t) - z(t)$, and $v(t)$ is the output, matrices D and J_c can be assumed null [17]. The augmented matrices in Equation 31 are written as function of the compensator leading to:

$$\begin{aligned}A &= \begin{bmatrix}A & 0\\ -GH & F\end{bmatrix}\\ B &= \begin{bmatrix}B\\ 0\end{bmatrix}\\ F &= \begin{bmatrix}0\\ J_c\end{bmatrix}\\ C &= \begin{bmatrix}C & 0\\ J_cH & 0\end{bmatrix}\\ H &= \begin{bmatrix}H & 0\end{bmatrix}\end{aligned} \tag{33}$$

Where the original matrices A, B and C, are product of the linearization of the aircraft model through small perturbation theory, see Appendix 7 which shows these matrices corresponding to the aircraft equilibrium point $v = 250m/s$ and $H = 5000m$. Finally, the control input of the system can be expressed as $u = -Ky$. Substituting the measured output $y(t)$ in the input we obtain the closed-loop control:

$$u = -Ky = -KCx - KFr \tag{34}$$

With K as the gain matrix $(m \times p)$ to be determined by mean of an optimization process. This is done minimizing a performance index J, to do this, it is necessary to define the matrices A_c and B_c of a Lyapunov equation (defined bellow in Equation 40). Substituting Equation 34 in Equation 31 we obtain:

$$\begin{aligned}\dot{x} &= Ax + Bu + Gr\\ &= (A - BKC)x + (G - BKF)r\\ &= A_c x + B_c r\end{aligned} \tag{35}$$

To solve the tracking problem of the total velocity V through elevator deflection, we define the state and output vectors respectively as $x = [V, \alpha, \Theta, q, \delta_p, \varepsilon]^T$ and $y = [V, \varepsilon]^T$. The ε variable represents the output of the integrator used to cancel the stationary error [17]. To make the simulations more realistic, an actuator for the elevator was modeled (δ_p). The actuator model implemented in this design was modeled in the state space as in Equation 36 as used in [16], the same model will be used in the UIR simulations.

$$\dot{\delta}_p = -20.2\delta_p + 20.2u_a \tag{36}$$

The actuator input u_a can be seen as the input voltage of the electro-hydraulic actuator and δ_p as the elevator deflection. Then, the augmented matrices can be written as shown in appendix 7. Matrix C represents the measured outputs (velocity V and tracking error ε). null matrix F indicates that the compensator output was not taken into account and H is the performance output of the problem. Finally, the control is written as function of the gain matrix and the feedback of total velocity V and tracking error ε, as showed in Equation 37.

$$u = -Ky = -\begin{bmatrix} K_V & K_\varepsilon \end{bmatrix} \begin{bmatrix} V \\ \varepsilon \end{bmatrix} \tag{37}$$

With K_V as the velocity feedback gain and K_ε the integral gain of the tracking error. Figure 1 shows the control loop to the tracking problem of total velocity of the Mirage III aircraft.

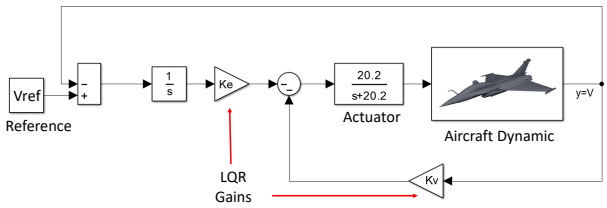

Fig. 1 LQR-control loop

The performance index for this problem is defined by Equation 38

$$J = \frac{1}{2}\int_0^\infty (x^T Qx + u^T Ru)dt \tag{38}$$

Matrices Q and R are chosen using the Bryson rule (in which Q and R depend on bounds imposed to the output to be controlled and bounds of the control itself). Once the augmented system and the matrices Q and R are defined, we proceed to determine numerically the initial gain matrix of the optimization process K_s, the main idea is to calculate the gains such that matrix A_c of Equation 35 is Hurwitz [7]. Then the K_s gains are used as initial condition to minimize the performance index J of Equation 38. It must be remembered that the dynamic optimization problem of solving Equation 38 can be transformed into an equivalent static one, easier to solve, resulting in a new performance index of the form (see book [17]):

$$J = \frac{1}{2}x^T(0)Px(0) \tag{39}$$

Where P is a matrix that needs to be solved from the Lyapunov Equation 40 that depends on the gain matrix K, for this reason a initial gain matrix K_s is computed before.

$$A_c^T P + PA_c + C^T K^T RKC + Q = 0 \tag{40}$$

Once P is determined, the performance index J is minimized using the *fmincon* function of MATLAB®. As previously mentioned, in order to compare this controller (LQR) with the UIR controller, the same reference velocity to be tracked is defined in both controllers. It is important to highlight that the optimization process consists of iteratively change the gains K in Equation 40 in order to the resulting P matrix be able to minimize the performance index J.

5 Numerical Simulations

The equilibrium points used as initial conditions for the simulations are listed in Table 2, this points belong to the flight envelope of the Mirage III aircraft. Point 1 is an intermediate point of the envelope, the matrices in appendix 7 correspond to this point. The reference velocity to be tracked consists of increasing the initial velocity in 4% for 20 seconds (between simulation time 10-30s)

in a "ramp type" path as will be seen in the next section.

Table 2 Equilibrium points.

Point	Altitude [m]	velocity [m/s]
1	5000	250
2	1524	134
3	1524	334
4	10668	208
5	10668	386

5.1 UIR controller

For the UIR controller, the relative degree analytically calculated was $\rho = 3$, matching with the relative degree used in the work of [3]. The controller parameters determined in section 3 are: $k_0^V = 9$, $K_1^V = 1$, $K_2^V = 2$ and $\mu_V = 2$, it is worth to mention that according to [5] the μ_V value does not have to be necessarily close to zero, it should be small enough to guarantee that the performance of the ideal SMC is achieved, simulations were accomplished using different μ_V values, $\mu_V = 2$ demonstrated a good relationship between tracking error and non-production of chattering (signal to measure how close we are from ideal SMC behavior). Once μ_V is chosen, the controller gain K_V is calculated using $K_V = \nu_V(\cdot) + q_V$ with $q_V = 2.1 k_0^V \mu_V > 0$, it must to be remembered that $\nu_V(\cdot)$ is the result of a maximizing function dependent on $|b(x)|$ (see Equation 16). The initial idea was to determine the maximum value of $\nu_V(\cdot)$ but it was not possible due to the huge function found and the absence of maximum values of some parameters as pitch rates (p,q,r) for exmaple. Finally, the controller gain K_V was found by a trial and error process and the final UIR controller, theoretically defined in Equation 26 will be as in Equation 41.

$$u_V^{UIR} = \delta_p^V = -0.002 sat\left(\frac{9\sigma_V + e_1^V + 2e_2^V + e_3^V}{2}\right) \tag{41}$$

In Figure 2 is shown the performance of the controller of Equation 41, it is worth mentioning that this controller showed to be effective in all the points of the flight envelope with the same gain K_V, dispensing the use of gain scheduling. It easy to check that points where altitude is higher, required more control amplitude (elevator deflection) to maintain a small tracking error, this can be explained by the fact that dynamic pressure is smaller, therefore, the control surface effectiveness is poorer. It can be highlighted that control deflections in Figure 2 are measure in relation to their equilibrium deflection (initial elevator deflection).

5.2 LQR controller

In order to determine matrices Q and R, the bounds imposed to the state to be controlled (Velocity) is $x_1^{max} = 12 m/s$ in relation to the equilibrium velocity, and the bound to the control (elevator deflection) is $u_1^{max} = [30° - (-30°)] = 60°$, then the matrices Q and R are shown in Equation 42 and the final gains after the optimization process for the points in Table 2 are presented in Table 3.

$$Q = \left[\frac{1}{12^2}\right]; \quad R = \left[\frac{1}{(60/57.29)^2}\right] \tag{42}$$

Table 3 LQR gains for all equilibrium points.

Point	Gain K_V	Gain K_ε
1	0.0272	-0.0269
2	0.0209	-0.0134
3	0.0450	-0.0310
4	0.0126	-0.0152
5	0.0229	-0.0360

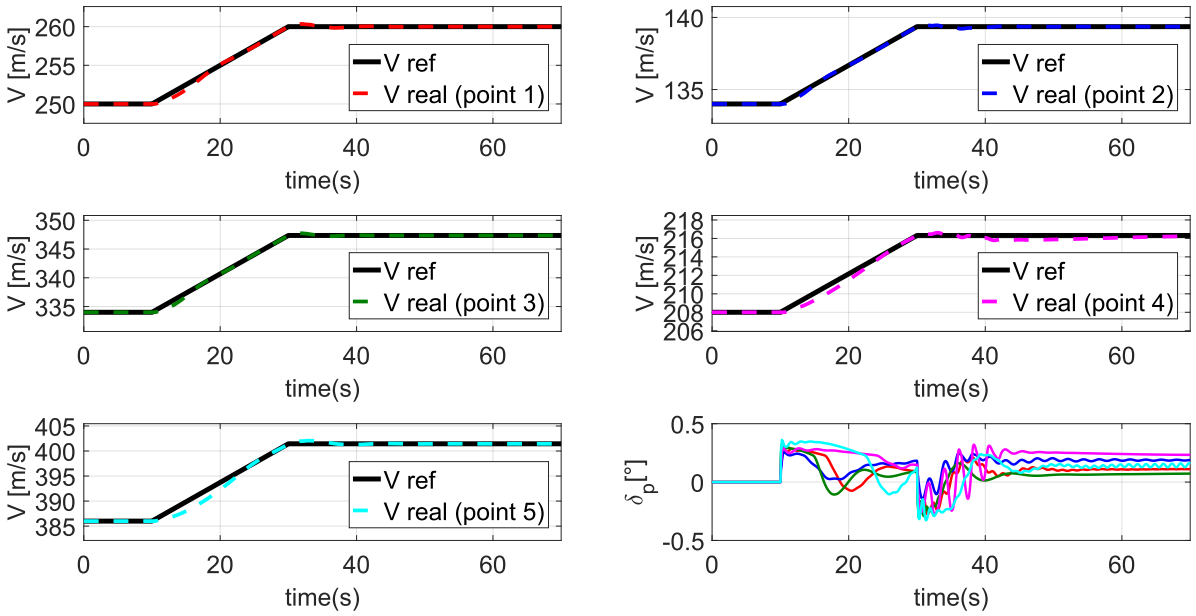

Fig. 2 Total velocity tracking (all points)- UIR

Then, the final LQR controller is composed by the combination of the Equations 37 and 40 leading to 43 (for point 1). In Figure 3 is shown the tracking performance of the LQR controller for total velocity in point 1, it is possible to see that the actual (or real) velocity track the reference with a small stationary error of approximately 0.5 m/s during the change of velocity and close to zero once settled down in the velocity of 260 m/s. Figure 4 illustrates the total velocity tracking for points 2 to 5 of the aircraft flight envelope, with the LQR controller gains of Table 3 previously calculate, results demonstrated a good performance of the controller.

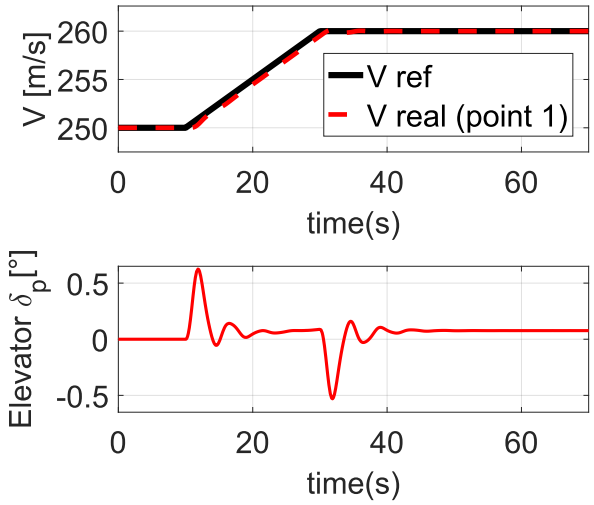

Fig. 3 Total velocity tracking (point 1)- LQR

$$u_V^{LQR} = \delta_p^V = -0.0272V + 0.0269\varepsilon \qquad (43)$$

5.3 Comparison UIR and LQR

A comparison of the performance between both controllers UIR and LQR is shown in Figure 5. Both controllers tried to achieve the reference output, it can be seen in Figure 6 that the tracking error using the UIR controller was smaller than the corresponding tracking error for the LQR controller during the velocity climb despite having higher peaks. With respect to the control, the UIR controller demanded less elevator amplitude than LQR controller. The tracking error response for both control techniques for points 2 to 5 have been plotted and showed in Figure 7, it can be noted that UIR provided a small error, especially in points 2 and 3 where the tracking error stays close to zero during velocity transition, despite in

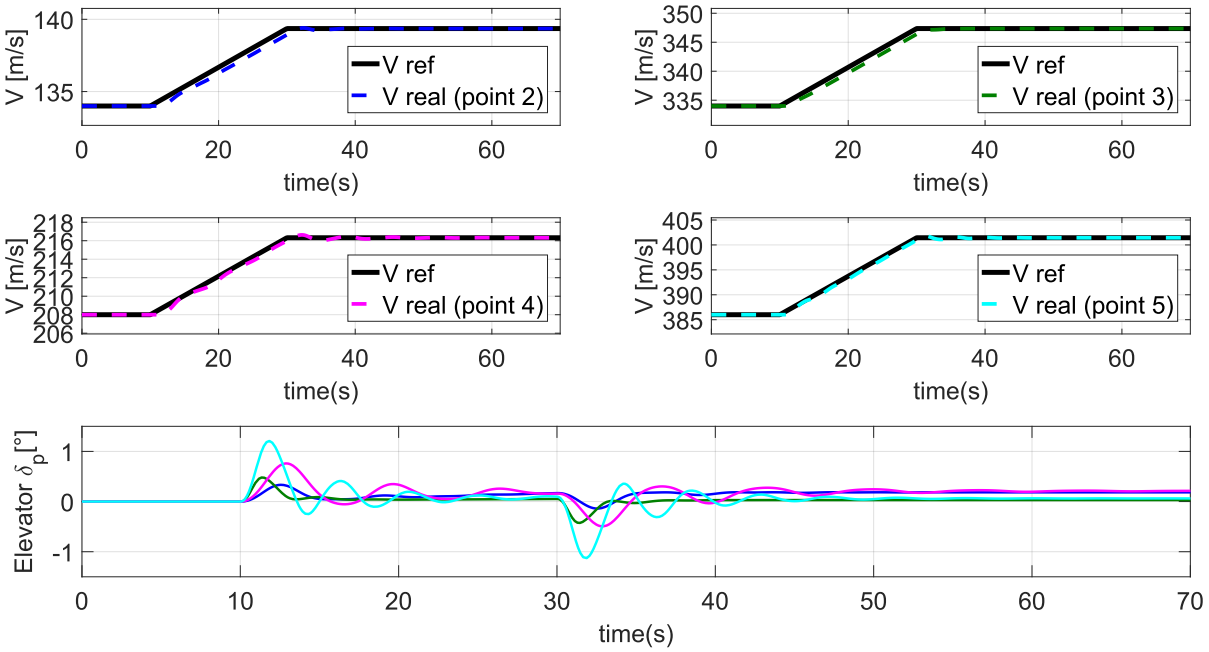

Fig. 4 Total velocity tracking (points 2 to 5)- LQR

points 4 and 5 the tracking error for LQR was smaller, its behavior was more oscillatory, this can be seen as more control activity.

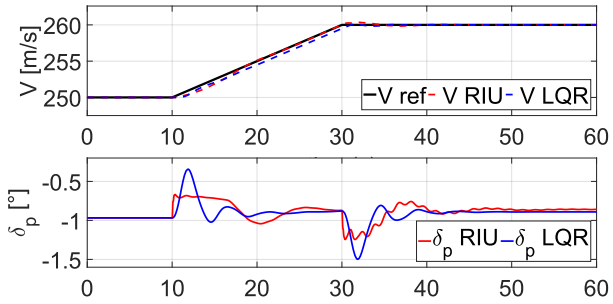

Fig. 5 Total velocity tracking (point 1)- UIR and LQR

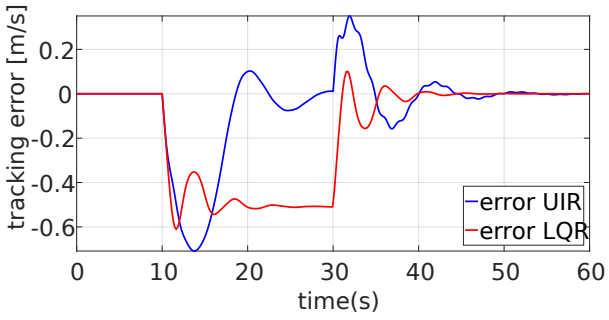

Fig. 6 Total tracking error (point 1)- UIR and LQR

6 Conclusions

An aircraft velocity hold autopilot was designed and successfully implemented to a fighter aircraft nonlinear model. Modern linear and nonlinear control techniques, LQR and UIR respectively were designed, both of them are error dependent. The analytic process to obtain and define the control parameters was developed, specific details were shown for the relatively new UIR technique. The tracking problem was formulated and solved using both techniques. Results demonstrated a better performance for the UIR technique providing less control activity (smaller elevator deflection and less oscillations) and smaller tracking errors during velocity transition (climb). It is worth to mention that UIR technique, since its conception, has had a little application in flight control, and this work represents an incentive to be implemented in more aircraft projects. Despite the LQR is one of the most used control technique at industry and its gain being calculated af-

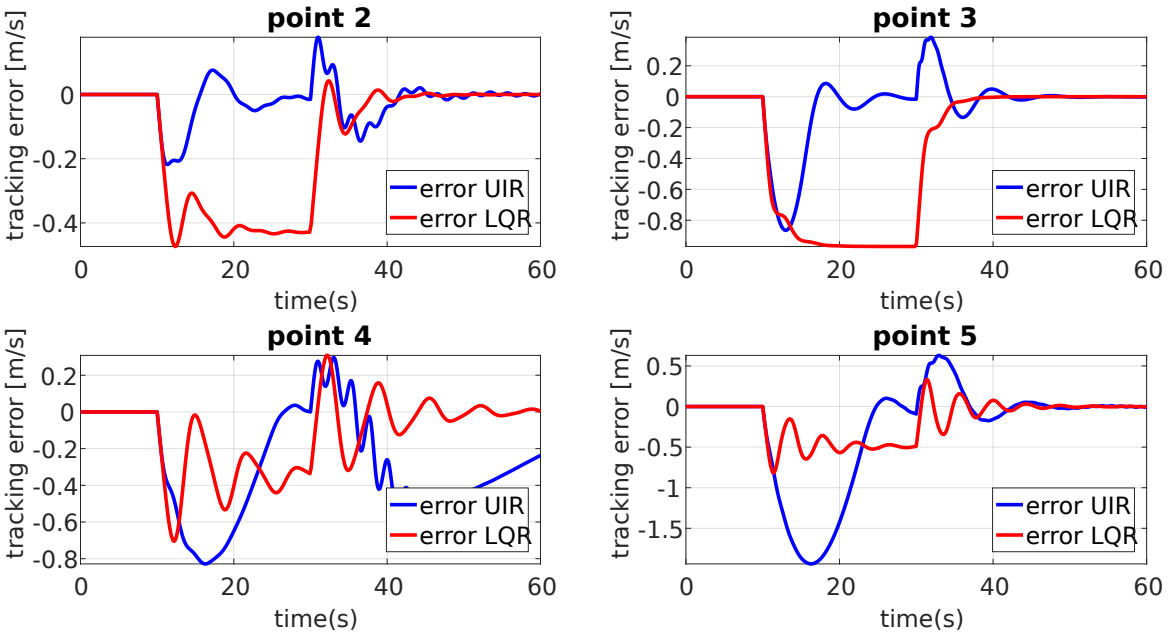

Fig. 7 Tracking error (points 2 to 5)- UIR and LQR

ter the optimization of a performance index, the UIR controller, even with a non-optimized gain demonstrated a better performance. Another advantage of the UIR, as expected, is the use of only one set of control parameters valid at the whole flight envelope (or at least in the 5 points tested) showing more robustness.

7 Appendix 1: Augmented matrices of LQR controller

Equations 44 and 45 are based on the linearization of the nonlinear model in equilibrium point 1 and then augmented with the LQR compensator and aircraft actuator dynamic.

$$A = \begin{bmatrix} -0.01 & -7.41 & -9.8 & 0 & -5.43 & 0 \\ -0.00 & -0.99 & 0 & 1 & -0.31 & 0 \\ 0 & 0 & 0 & 1 & 0 & 0 \\ 0 & -13.69 & 0 & -0.67 & -36.24 & 0 \\ 0 & 0 & 0 & 0 & -20.2 & 0 \\ -1 & 0 & 0 & 0 & 0 & 0 \end{bmatrix} \quad (44)$$

$$\begin{aligned} B &= \begin{bmatrix} 0 & 0 & 0 & 0 & 20.2 & 0 \end{bmatrix}^T \\ C &= \begin{bmatrix} 1 & 0 & 0 & 0 & 0 & 0 \\ 0 & 0 & 0 & 0 & 0 & 1 \end{bmatrix} \\ G &= \begin{bmatrix} 0 & 0 & 0 & 0 & 0 & 1 \end{bmatrix}^T \\ H &= \begin{bmatrix} 1 & 0 & 0 & 0 & 0 & 0 \end{bmatrix} \\ F &= \begin{bmatrix} 0 \\ 0 \end{bmatrix} \end{aligned} \quad (45)$$

8 References

References

[1] Samir Bouabdallah, Andre Noth, and Roland Siegwart. Pid vs lq control techniques applied to an indoor micro quadrotor. In *Intelligent Robots and Systems, 2004.(IROS 2004). Proceedings. 2004 IEEE/RSJ International Conference on*, volume 3, pages 2451–2456. IEEE, 2004.

[2] André Luís Da Silva. Procedimento de projeto de leis de controle de vôo de aeronaves utilizando o controle à estrutura var-

iável. Master's thesis, Instituto Tecnológico de Aeronáutica, 2007.

[3] Marcelo Santiago de Sousa, Pedro Paglione, Flávio Luiz Cardoso Ribeiro, and Roberto Gil Annes da Silva. Use of universal integral regulator to control the flight dynamics of flexible airplanes. 2013.

[4] Dagfinn Gangsaas, John Hodgkinson, Clay Harden, Nomaan Saeed, and Kaiming Chen. Multidisciplinary control law design and flight test demonstration on a business jet. In *AIAA Guidance, Navigation and Control Conference and Exhibit*, page 6489, 2008.

[5] Hassan K Khalil. Universal integral controllers for minimum-phase nonlinear systems. *IEEE Transactions on automatic control*, 45(3):490–494, 2000.

[6] HK Khalil. Improved performance of universal integral regulators. *Journal of optimization theory and applications*, 115(3):571–586, 2002.

[7] Katsuhiko Ogata and Yanjuan Yang. *Modern control engineering*, volume 4. Prentice hall India, 2002.

[8] Jyoti Ohri et al. Ga tuned lqr and pid controller for aircraft pitch control. In *Power Electronics (IICPE), 2014 IEEE 6th India International Conference on*, pages 1–6. IEEE, 2014.

[9] Heri Purnawan, Eko Budi Purwanto, et al. Design of linear quadratic regulator (lqr) control system for flight stability of lsu-05. In *Journal of Physics: Conference Series*, volume 890, page 012056. IOP Publishing, 2017.

[10] V Rajeswari and L Padma Suresh. Comparative assessment of the performances of lqr and smc methodologies in the control of longitudinal axis of aircraft. In *Proceedings of the International Conference on Soft Computing Systems*, pages 481–490. Springer, 2016.

[11] Obaid Ur Rehman, Barış Fidan, and Ian R Petersen. Uncertainty modeling and robust minimax lqr control of multivariable nonlinear systems with application to hypersonic flight. *Asian Journal of Control*, 14(5):1180–1193, 2012.

[12] Sridhar Seshagiri and Hassan K Khalil. Robust output feedback regulation of minimum-phase nonlinear systems using conditional integrators. *Automatica*, 41(1):43–54, 2005.

[13] Christopher M Shearer. *Coupled nonlinear flight dynamics, aeroelasticity, and control of very flexible aircraft.* PhD thesis, 2006.

[14] Jean-Jacques E Slotine, Weiping Li, et al. *Applied nonlinear control*, volume 199. Prentice hall Englewood Cliffs, NJ, 1991.

[15] MS Sousa. Projeto de um sistema de controle de uma aeronave de estabilidade variável usando o método do modelo de referência. Master's thesis, Technological Institute of Aeronautics-ITA São José dos Campos, 2005.

[16] MS Sousa. *Modelagem, simulação e controle não linear de aviões muito flexíveis*. PhD thesis, Technological Institute of Aeronautics-ITA São José dos Campos, 2013.

[17] Brian L Stevens and Frank L Lewis. Aircraft control and simulation. 2003.

[18] Ilhan Tuzcu. *Dynamics and Control of Flexible Aircraft*. PhD thesis, Virginia Tech, 2001.

[19] Haojian Xu, Maj D Mirmirani, and Petros A Ioannou. Adaptive sliding mode control design for a hypersonic flight vehicle. *Journal of guidance, control, and dynamics*, 27(5):829–838, 2004.

9 Acknowledgments

The authors would like to acknowledge the financial support from the Brazilian agency FAPEMIG-Foundation of Support Research of the State of Minas Gerais.

10 Contact Author Email Address

Corresponding author: Yohan Díaz Email: yohan.g8@unifei.edu.br

Copyright Statement